



Published in final edited form as:

*J Am Chem Soc.* 2013 February 6; 135(5): 1749–1759. doi:10.1021/ja307710d.

## Nonribosomal Propeptide Precursor in Nocardicin A Biosynthesis Predicted from Adenylation Domain Specificity Dependent on the MbtH Family Protein NocI

Jeanne M. Davidsen, David M. Bartley<sup>1</sup>, and Craig A. Townsend\*

Department of Chemistry, Johns Hopkins University, Baltimore, Maryland 21218

### Abstract

Nocardicin A is a monocyclic  $\beta$ -lactam isolated from the actinomycete *Nocardia uniformis* that shows moderate antibiotic activity against a broad spectrum of Gram-negative bacteria. The monobactams are of renewed interest due to emerging Gram-negative strains resistant to clinically available penicillins and cephalosporins. Like isopenicillin N, nocardicin A has a tripeptide core of nonribosomal origin. Paradoxically, the nocardicin A gene cluster encodes two nonribosomal peptide synthetases (NRPSs), NocA and NocB, predicted to encode five modules pointing to a pentapeptide precursor in nocardicin A biosynthesis, unless module skipping or other non-linear reactions are occurring. Previous radiochemical incorporation experiments and bioinformatic analyses predict the incorporation of *p*-hydroxy-L-phenylglycine (L-*p*HPG) into positions 1, 3, and 5 and L-serine into position 4. No prediction could be made for position 2. Multi-domain constructs of each module were heterologously expressed in *Escherichia coli* for determination of the adenylation domain (A-domain) substrate specificity using the ATP/PPi exchange assay. Three of the five A-domains, from modules 1, 2, and 4, required the addition of stoichiometric amounts of MbtH family protein NocI to detect exchange activity. Based on these analyses, the predicted product of the NocA+NocB NRPSs is L-*p*HPG-L-Arg-D-*p*HPG-L-Ser-L-*p*HPG, a pentapeptide. Despite being flanked by nonproteinogenic amino acids, proteolysis of this pentapeptide by trypsin yields two fragments from cleavage at the C-terminus of the L-Arg residue. Thus, a proteolytic step is likely involved in the biosynthesis of nocardicin A, a rare but precedented editing event in the formation of nonribosomal natural products which is supported by the identification of trypsin-encoding genes in *N. uniformis*.

### Introduction

The peptide core of many bioactive natural products, such as the antibiotics penicillin, vancomycin, and daptomycin, is biosynthesized by large modular proteins known as nonribosomal peptide synthetases (NRPS).<sup>1</sup> Interactions between NRPSs and other proteins are essential for overall catalytic function. NRPS proteins must interact with 4'-phosphopantethieryl transferases (PPTase) that catalyze the transfer of a phosphopantethieryl side chain from coenzyme A to the active site serine residue of each peptidyl carrier or thiolation (T) domain of the NRPS, converting the *apo*-NRPS to its *holo*-form.<sup>1,2</sup> In addition, there are increasing numbers of examples of associated biosynthetic proteins known to catalyze reactions, typically oxidations and halogenations, on T-domain

\*Corresponding author. Mailing address: Department of Chemistry, Johns Hopkins University, Baltimore, MD 21218. Phone: (410) 516-7444. Fax: (410) 261-1233. ctownsend@jhu.edu.

<sup>1</sup>Current address: Department of Chemistry, Adrian College, Adrian, MI 49221

Supporting Information Available

Figure containing HPLC chromatograms and mass analysis for the trypsinolysis reaction of pentapeptide L-*p*HPG-L-Arg-D-*p*HPG-L-Ser-L-*p*HPG and protein sequence alignments. This information is available free of charge via the internet at <http://pubs.acs.org>.

tethered substrates.<sup>3,4</sup> At the N- and C-termini of paired NRPS proteins, “COM domains”, consisting of  $\alpha$ -helical recognition units, are points of mutual interaction linking the product assembly reactions on each.<sup>5</sup> The importance of NRPS interaction with one or more auxiliary proteins for optimal activity is particularly well exemplified by recent discoveries that identify the crucial role of the MbtH family of proteins. The MbtH family comprise a group of relatively small proteins (~8–9 KDa) often found embedded in biosynthetic clusters for nonribosomal peptide-derived secondary metabolites. They are collectively named for the protein identified in the mycobactin biosynthetic cluster of *Mycobacterium tuberculosis*.<sup>6</sup> *In vivo* studies of *Streptomyces coelicolor* A3(2) concluded that MbtH family proteins, CchK associated with the coelichelin gene cluster and CdaX associated with the calcium-dependent antibiotic (CDA) gene cluster, are indispensable for production of these secondary metabolites.<sup>7</sup> Another study demonstrated that heterologous expression of chlorobiocin in *S. coelicolor* M512 was barely detectable upon the removal of all MbtH protein coding regions but complementation with *mbtH* genes *cchK*, *cdaX*, *cloY*, or *couY* (from the related coumermycin gene cluster) substantially restored production.<sup>7,8</sup>

Despite the prevalence of MbtH encoding genes in NRPS-containing gene clusters and *in vivo* studies demonstrating their importance and structure determinations,<sup>9,10</sup> the role of these proteins in nonribosomal peptide biosynthesis remained unclear until the ATP/PPi exchange activity of the NRPS protein VbsS was found to be dependent on its co-expression with VbsG, an MbtH protein encoded next to the NRPS in the vicibactin gene cluster.<sup>11</sup> A minimal NRPS module is three domains – an adenylation (A) domain, a thiolation (T) domain, and a condensation (C) domain. A-domains activate their cognate substrate, typically an L- $\alpha$ -amino acid, by catalyzing the adenylation of the carboxylate moiety by reaction with ATP. This reaction is usually reversible and can be monitored by an ATP/PPi exchange assay. The activated substrate reacts with the terminal thiol group of the pantethenyl side chain of the T-domain, forming a thioester. C-domains catalyze peptide bond formation between the free amino group of the upstream T-domain tethered aminoacylthioester with the downstream T-domain thioester. NRPSs usually terminate with a thioesterase (TE) domain, which catalyzes the release of the nascent peptide chain by hydrolysis or macrocyclization.

Several bioinformatic algorithms have been developed for substrate prediction of A-domains. The first algorithms were based on the crystal structure of PheA, the L-phenylalanine activating domain of the gramicidin NRPSs.<sup>12</sup> Structure studies of PheA show the substrate binding pocket and ATP binding region at the interface of the N-terminal and C-terminal domains of the enzyme. A-domain substrate prediction algorithms were derived by correlating the residues directly lining the substrate binding pocket to its cognate substrate.<sup>13,14</sup> More recent A-domain prediction algorithms have used transductive support vector machines (TSVMs) or hidden Markov Model (HMM) methodologies to improve prediction capabilities.<sup>15–17</sup>

The activation of ATP/PPi exchange activity in VbsS by VbsG suggests the MbtH protein interacts with the A domain of VbsS. The contribution of MbtH homologues VioN, CmnN, and PacJ to the activity of NRPSs involved in the biosynthesis of viomycin, capreomycin and pacidamycin, respectively, were subsequently reported.<sup>18,19</sup> CmnN and VioN were found to be necessary to activate the ATP/PPi exchange reactions in the  $\beta$ -lysine activating modules of CmnO and VioO and modules 1 and 2 from CmnA, but are not required for ATP/PPi exchange in the A-domains of NRPSs CmnF and CmnG. PacJ is required for activation of ATP/PPi exchange in PacL. The mechanism for A-domain activation by MbtH proteins remains unclear. Kinetic measurements of the NovH tyrosine activating domain in novobiocin biosynthesis indicated that the  $K_m$  and the turnover number measured for NovH

were dissimilar when paired with different but complementary MbtH proteins CloY and YbdZ.<sup>20</sup>

Nocardicin A is the most potent antibiotic of the monobactam nocardicins isolated from *N. uniformis* subsp. *tsuyamanensis* ATCC 21806, with activity against gram-negative bacteria. Nocardicin A has also been isolated from other actinomycetes, including *Actinosynnema mirum*.<sup>21</sup> The genus *Actinosynnema* is characterized by the formation of synnemata from the substrate mycelium, at the tip of which, zoospores are produced.<sup>22</sup> Classical morphological comparison of *N. uniformis* ATCC 21806 to *A. mirum* strain NR 0364 revealed a high degree of similarity in the formation of synnemata and zoospores suggesting that it should be reclassified into the *Actinosynnema* genus.<sup>21</sup>

While both *A. mirum* and *N. uniformis* produce nocardicin A and have nearly identical gene clusters, the biosynthetic pathway has only been studied in *N. uniformis*. The structures of all the nocardicins isolated from *N. uniformis* contain a tripeptide core known to be derived from two units of *p*-hydroxy-L-phenylglycine (L-*p*HPG) and one unit of L-Ser.<sup>23</sup> While a three module NPRS would be expected in the nocardicin A gene cluster, two NRPSs, NocA and NocB, together containing five modules were found.<sup>24</sup> Recent *in vivo* mutagenesis experiments indicate that each of these five modules is essential, demonstrating that module skipping is not likely occurring and implying the formation of pentapeptide precursor in nocardicin A biosynthesis by the conventional linear paradigm.<sup>24</sup> Determination of each A-domain substrate specificity would provide the identity of this putative pentapeptide and may suggest mechanisms by which subsequent truncation occurs to form the tripeptide backbone of the nocardicins. Bioinformatic algorithms have predicted L-*p*HPG to be the preferred substrate for A1, A3, and A5 and L-Ser to be the preferred substrate for A4.<sup>13</sup> The substrate specificity for A2 has been more problematic with low confidence predictions ranging from L-ornithine or L- $\delta$ -*N*-hydroxyornithine,<sup>24</sup> “a large amino acid such as L-Orn, L-Lys or L-Arg”, a hydrophilic amino acid, L-Asp, L-Asn, L-Glu, or L-Gln, or L-Arg.<sup>15,25</sup> The inability to obtain clear experimental data for A2 has prevented identification of the presumed pentapeptide and left unknown whether the tripeptide backbone of nocardicin A originates from modules 1–3 or 3–5.

Among the proteins encoded by the nocardicin A biosynthetic cluster, NocI, a small 74 amino acid protein, shows clear homology to the MbtH family of proteins, and 2.3 kbp upstream of the cluster, a 73 amino acid paralog encoded by *nocP* is found. In this study, we report MbtH protein NocI is required for ATP/PPi exchange to be observed in three of the five A-domains of NocA and NocB. Surprisingly, the MbtH protein encoded just upstream of the cluster, NocP, was found to only partially complement NocI. The A-domain•NocI/NocP protein interaction was further characterized by co-expression studies. HPLC and binding analyses of dependent modules co-expressed with NocI indicate a 1:1 stoichiometry. Determining the function of NocI was requisite to experimentally demonstrating the identities of the amino acids recognized and activated by each module of NocA and NocB. As a result, a pentapeptide precursor can now be proposed for nocardicin A biosynthesis, as well as possible mechanisms for proteolysis to a tripeptide later in the biosynthetic pathway.

## Results

### Adenylation Domain Specificities of NocA and NocB

Heterologous expression of a multidomain construct from each module of NocA and NocB in *Escherichia coli* (*E. coli*) was pursued so that the substrate specificity could be experimentally determined for each A-domain using the standard ATP/PPi exchange assay. For all modules, except module 2, each construct was cloned into pET28b(+) for expression of C-terminal His<sub>6</sub> fusion proteins in *E. coli* BL21(DE3) Rosetta 2 cells and purification by

NTA affinity chromatography and Q-Sepharose ion exchange chromatography. Yields typically ranged from 0.5–1 mg protein/L culture. Because this expression protocol failed for several constructs of module 2, the A<sub>2</sub>T<sub>2</sub>-His<sub>6</sub> coding sequence was cloned into pMALc2x for expression of an N-terminal maltose binding protein (MBP) fusion protein. Heterologous expression of MBP-A<sub>2</sub>T<sub>2</sub>-His<sub>6</sub> in *E. coli* BL21(DE3) Rosetta 2 and isolation by NTA affinity chromatography yielded 2–3 mg protein/L culture. Protein products were confirmed by MALDI analysis of trypsin digests.

Bioinformatic analysis of the A-domains of modules 1, 3 and 5 predicted L-*p*HPG to be their preferred substrate although protein sequence alignment of these three A-domains highlights a long linker region between motifs 2 and 3 in the A1 domain that is not found in the A3 or A5 domains.<sup>24</sup> The ATP/PPi exchange assay results for A<sub>1</sub>T<sub>1</sub>-His<sub>6</sub>, A<sub>3</sub>T<sub>3</sub> E<sub>3</sub>C<sub>4</sub>-His<sub>6</sub> and C<sub>5</sub>A<sub>5</sub>T<sub>5</sub>TE-His<sub>6</sub> are shown in Figure 1A. Very strong ATP/PPi exchange was observed in the presence of L-*p*HPG for these three modules with a marked lack of activity for any other amino acid substrate. Although some exchange above background was observed with D-*p*HPG as substrate (ca. 6% relative to L-*p*HPG), this observed activity is likely the result of a small L-isomer impurity. It should be noted that no exchange activity was observed for closely related analogues of *p*HPG such as L-phenylglycine (PG), D-PG, D/L-4-fluorophenylglycine (FPG) or D/L-4-chlorophenylglycine (CIPG), a further indication of the high specificity of these A-domains.

For the present discussion, however, it is important to note that despite the similarity of the amino acid binding pockets of A1, A3 and A5, ATP/PPi exchange in A<sub>1</sub>T<sub>1</sub>-His<sub>6</sub> was only observed in the presence of the MbtH proteins NocI or NocP. Of the three L-*p*HPG activating modules, ATP/PPi exchange was dependent on stoichiometric amounts of MbtH protein only in A<sub>1</sub>T<sub>1</sub>-His<sub>6</sub>. The addition of NocI to A<sub>3</sub>T<sub>3</sub> E<sub>3</sub>C<sub>4</sub>-His<sub>6</sub> and C<sub>5</sub>A<sub>5</sub>T<sub>5</sub>TE-His<sub>6</sub> had no effect on the ATP/PPi exchange reaction under identical experimental conditions.

The substrate binding pocket of the A4 domain in NocB was predicted to activate L-serine by several algorithms and was consistent with past experiments that established the β-lactam ring of nocardicin A is derived from L-serine.<sup>23</sup> Initial ATP/PPi exchange assays of A<sub>4</sub>T<sub>4</sub>-His<sub>6</sub> failed to demonstrate any significant activity in the presence of any amino acid. As observed in experiments with A<sub>1</sub>T<sub>1</sub>-His<sub>6</sub>, A<sub>4</sub>T<sub>4</sub>-His<sub>6</sub> was also dependent on the presence of stoichiometric amounts of NocI for the observation of ATP/PPi exchange with its preferred substrate, L-serine as shown in Figure 1B.

Substrate determination for the A2 domain has been the most difficult to achieve of the five modules, as noted earlier. Recently, the A6 domain of the lysobactin NRPS was characterized to activate L-Arg, independent of the presence of a MbtH protein.<sup>26</sup> A2 shares the 8 residue L-Arg binding pocket signature with this lysobactin A-domain, as well as showing good overall similarity to it (40.2% identical, 55.8% similar). Upon expression and purification of MBP-A<sub>2</sub>T<sub>2</sub>-His<sub>6</sub>, initial ATP/PPi exchange experiments conducted under conditions used to characterize A<sub>1</sub>T<sub>1</sub>-His<sub>6</sub>, A<sub>3</sub>T<sub>3</sub> E<sub>3</sub>C<sub>4</sub>-His<sub>6</sub>, A<sub>4</sub>T<sub>4</sub>-His<sub>6</sub> and C<sub>5</sub>A<sub>5</sub>T<sub>5</sub>TE-His<sub>6</sub> demonstrated only weak exchange activity and poor selectivity in the presence of small hydrophobic amino acids such as L-Val, L-Leu, and L-Ile and no exchange activity for L-Arg. As depicted in Figure 2A, the observation of L-Arg dependent ATP/PPi exchange was only observed under altered assay conditions<sup>26</sup> involving a 10-fold higher concentration of protein, conducting experiments at 30 °C instead of room temperature (~23 °C), and the addition of a 2-fold excess of NocI to the assay. Of note, under these conditions significant ATP/PPi exchange was also observed for the hydrophobic amino acids L-Val, L-Leu, L-Ile, and L-Phe, but this activity was not dependent on the addition of the MbtH protein, NocI. The dramatic activation of ATP/PPi exchange by NocI in the presence of L-Arg compared to the small hydrophobic amino acids is seen in a difference plot (Figure 2B). Also, unlike

the lysobactin A6 domain, ATP/PPi exchange activity by MBP-A<sub>2</sub>T<sub>2</sub>-His<sub>6</sub> was not observed for D-Arg nor was ATP/PPi exchange activity observed for similar amino acids predicted from bioinformatics such as L-ornithine, L- $\delta$ -N-hydroxyornithine, L- $\delta$ -N-acetyl- $\delta$ -N-hydroxyornithine, or L-Lys.

### Interaction of MbtH Proteins NocI and NocP with Nocardicin A-domains

To understand further its interaction with each nocardicin module, NocI was cloned into pCDFDuet for heterologous expression as an N-terminal His<sub>6</sub> fusion protein as well as an untagged protein in *E. coli*. In addition, untagged NocI for *in vitro* experiments was prepared by heterologous expression of NocI fused to an intein attached to a chitin binding domain (CBD) tag followed by binding to chitin-binding affinity resin and cleavage of the CBD tag from NocI with DTT. The rate of ATP/PPi exchange as a function of NocI (untagged) concentration for 0.5  $\mu$ M concentrations of A<sub>1</sub>T<sub>1</sub>-His<sub>6</sub> and A<sub>4</sub>T<sub>4</sub>-His<sub>6</sub> is shown in Figure 3. Although the overall exchange rate is much higher for A<sub>1</sub>T<sub>1</sub>-His<sub>6</sub> compared to A<sub>4</sub>T<sub>4</sub>-His<sub>6</sub>, both hyperbolic curves plateau at  $\sim$  2  $\mu$ M NocI and have  $K_m$  values of 0.41  $\mu$ M and 0.59  $\mu$ M, respectively. In a similar experiment with A<sub>3</sub>T<sub>3</sub> E<sub>3</sub>C<sub>4</sub>-His<sub>6</sub> and C<sub>5</sub>A<sub>5</sub>T<sub>5</sub>TE-His<sub>6</sub>, NocI had no effect on the rate of ATP/PPi exchange of their preferred substrate L-pHPG. This observation was supported by analysis of the ATP/PPi exchange reaction for proteins isolated from an A<sub>3</sub>T<sub>3</sub> E<sub>3</sub>C<sub>4</sub>-His<sub>6</sub> – A<sub>4</sub>T<sub>4</sub>-His<sub>6</sub> co-expression experiment. Addition of His<sub>6</sub>-NocI to the assay greatly enhanced ATP/PPi exchange activity observed in the presence of L-Ser but showed little effect on the activity observed in the presence of L-pHPG.

To characterize further the interaction between each module and NocI, untagged NocI was co-expressed with each C-terminally labeled His<sub>6</sub> module protein. Following expression, the individual modules were isolated using the standard NTA affinity isolation protocol. SDS-PAGE analysis suggested that untagged NocI co-eluted (or was pulled down) by A<sub>1</sub>T<sub>1</sub>-His<sub>6</sub>, MBP-A<sub>2</sub>T<sub>2</sub>-His<sub>6</sub> and A<sub>4</sub>T<sub>4</sub>-His<sub>6</sub>, indicating strong interaction. This interaction was not observed during the purifications of A<sub>3</sub>T<sub>3</sub> E<sub>3</sub>C<sub>4</sub>-His<sub>6</sub> or C<sub>5</sub>A<sub>5</sub>T<sub>5</sub>TE-His<sub>6</sub> co-expressed with NocI. For a more quantitative evaluation, the final eluant for each co-expression reaction was denatured by the addition of urea and analyzed by HPLC to confirm the presence of NocI and estimate the module: NocI stoichiometry. The chromatogram and SDS-Page gel for the A<sub>4</sub>T<sub>4</sub>-His<sub>6</sub> – NocI co-expression are shown in Figure 4. As expected owing to its smaller size, NocI elutes first followed much later by A<sub>4</sub>T<sub>4</sub>-His<sub>6</sub>. Based on the area of each peak and the molar absorptivity of each protein calculated by Vector NTI, the A<sub>4</sub>T<sub>4</sub>-His<sub>6</sub>:NocI and A<sub>1</sub>T<sub>1</sub>-His<sub>6</sub>:NocI stoichiometric ratios were each calculated to be 1:1. The observation of a 1:1 stoichiometric relationship is consistent with the shape of the activity curves shown in Figure 3. Due to the complexity of the HPLC chromatogram, the stoichiometry of the MBP-A<sub>2</sub>T<sub>2</sub>-His<sub>6</sub> – NocI co-expression could not be confidently determined. Chromatograms for the co-expression of A<sub>3</sub>T<sub>3</sub> E<sub>3</sub>C<sub>4</sub>-His<sub>6</sub> – NocI and C<sub>5</sub>A<sub>5</sub>T<sub>5</sub>TE-His<sub>6</sub> – NocI failed to show any peak in the NocI region, consistent with SDS-PAGE analysis and in keeping with the absence of a strong binding between A3 or A5 with NocI.

The ability to reconstitute the activity of the A<sub>1</sub>T<sub>1</sub>-His<sub>6</sub>•NocI and A<sub>4</sub>T<sub>4</sub>-His<sub>6</sub>•NocI co-expressed proteins by combinations of individually expressed NocI, A<sub>1</sub>T<sub>1</sub>-His<sub>6</sub>, and A<sub>4</sub>T<sub>4</sub>-His<sub>6</sub> was also investigated, based on the HPLC response factors for each protein. The activity of reconstituted A<sub>4</sub>T<sub>4</sub>-His<sub>6</sub> and NocI was  $\sim$ 50% of the co-expressed A<sub>4</sub>T<sub>4</sub>-His<sub>6</sub>•NocI sample. For A<sub>1</sub>T<sub>1</sub>-His<sub>6</sub>, the activity of the reconstituted proteins was  $\sim$ 70% of the co-expressed A<sub>1</sub>T<sub>1</sub>-His<sub>6</sub>•NocI sample.

To investigate the ability of an MbtH family protein generated outside the nocardicin cluster to complement NocI, NocP was heterologously expressed in *E. coli* as an N-terminal His<sub>6</sub> fusion protein from pET28b(+) and as an untagged form from pCDFDuet. Several

experiments were carried out to compare the activity of His<sub>6</sub>-NocI to His<sub>6</sub>-NocP with A<sub>1</sub>T<sub>1</sub>-His<sub>6</sub>, MBP-A<sub>2</sub>T<sub>2</sub>-His<sub>6</sub> and A<sub>4</sub>T<sub>4</sub>-His<sub>6</sub>. Interestingly, His<sub>6</sub>-NocP activated ATP/PPi exchange activity in A<sub>1</sub>T<sub>1</sub>-His<sub>6</sub> and A<sub>4</sub>T<sub>4</sub>-His<sub>6</sub>, but not in MBP-A<sub>2</sub>T<sub>2</sub>-His<sub>6</sub>. Furthermore, analysis of the co-expression product of NocP (untagged) with MBP-A<sub>2</sub>T<sub>2</sub>-His<sub>6</sub> by HPLC indicated that NocP does not form a strong interaction with MBP-A<sub>2</sub>T<sub>2</sub>-His<sub>6</sub> yet NocI was pulled down by MBP-A<sub>2</sub>T<sub>2</sub>-His<sub>6</sub>. Together, these results indicate that NocP cannot fully complement NocI.

### Phylogenetic Analysis of *N. uniformis* ATCC 21806

To evaluate the phylogenetic similarity of *N. uniformis* to *A. mirum*, 16S rDNA was amplified from *N. uniformis* for sequencing and submitted to GenBank for comparison. The 16S rDNA (1508 nt) isolated from *N. uniformis* was found to be identical to *A. mirum* 16S rDNA (GenBank accession number CP001630.1) except for one polymorphism and are thus identical based on standard classification criteria.<sup>27,28</sup>

### Genome Mining for Trypsin Proteases in *A. mirum*

The predicted pentapeptide formed by NocA + NocB, L-*p*HPG-L-Arg-D-*p*HPG-L-Ser-L-*p*HPG requires trimming at the C-terminus of L-Arg during nocardicin A biosynthesis. Trypsins specifically cleave peptides at the C-terminus of L-Lys and L-Arg and have been isolated from bacteria as well as mammals.<sup>29</sup> However, BLASTP<sup>30</sup> analysis of the *A. mirum* complete genome revealed at least five probable trypsins, three of which have 38% identity 50% similarity to well characterized trypsins from *Streptomyces griseus* and *Saccharopolyspora erythraeus*.<sup>31,32</sup>

To confirm the presence of the trypsin encoding genes mined from the *A. mirum* genome in our strain, three trypsin proteases, ACU39320, ACU39665, and ACU39678, were selected for PCR amplification and sequence comparison. All three were successfully amplified from *N. uniformis* gDNA and confirmed by sequencing analysis to be identical to the corresponding *A. mirum* genes.

### Trypsin Proteolysis of Pentapeptide Precursor

The predicted product of the nocardicin NRPSs, L-*p*HPG-L-Arg-D-*p*HPG-L-Ser-L-*p*HPG, was purchased for evaluation. HPLC analysis of a pentapeptide trypsin reaction mixture showed the disappearance of the pentapeptide peak and the corresponding appearance of two new peaks with retention times significantly shorter than the starting material. (Supplemental Information Figure S1.) LC-MS/TOF analysis of the earliest eluting peak indicated a mass of 324.17 Da, which corresponds to the (M+H) of the L-*p*HPG-L-Arg dipeptide. The second peak has a mass of 404.15 Da consistent with the (M+H) of the predicted D-*p*HPG-L-Ser-L-*p*HPG tripeptide. Thus, this analysis indicates complete cleavage at the C-terminus of the L-Arg residue, as expected for trypsinolysis, despite its being flanked by two nonproteinogenic amino acids, one in the D-configuration.

## Discussion

NRPS A-domains constitute a sub-family of the ANL superfamily of adenylating enzymes, which also includes acyl and aryl CoA synthetases and firefly luciferase. ANL enzymes catalyze two reactions, the adenylation of a substrate carboxylate to form a high energy acyl-AMP intermediate followed by an acyl substitution reaction with the pantetheinyl side chain of a T-domain in the NRPS A-domain subfamily, reaction with CoA by members of the acyl and aryl CoA synthetases subfamily, or oxidative decarboxylation followed by the generation of light in the firefly luciferase subfamily.<sup>33</sup> Structure studies of the PheA domain, the initial A-domain in gramicidin S synthetase, show a two-domain structure with

a larger N-terminal domain (~430 residues) and a smaller C-terminal domain (~100 residues) with a connecting loop (A8 loop) between the two domains – a theme repeated throughout the ANL superfamily.<sup>12</sup> The PheA domain, crystallized with phenylalanine and AMP in the active site, is in the adenylation conformation, in which the conserved and essential A10 lysine forms hydrogen bonds with the oxygen atom in the ribose ring and the 5' bridging oxygen of AMP and the carboxylate oxygen of phenylalanine.<sup>12</sup> The alternation of conformational states during the catalytic cycle of the A-domain was first supported by crystal structure studies of DltA, a D-alanyl carrier protein ligase from *Bacillus cereus* that catalyzes the adenylation and thioesterification reaction of D-alanine in cell wall biosynthesis, which has been captured in several conformations.<sup>34–36</sup> This model is supported by recent crystal structure studies of PA1221, an two-domain (A-T) NRPS in both the adenylation and thioester-forming conformations.<sup>37</sup> Experimental evidence suggests that ANLs undergo a major ~140° conformational change between the adenylation and thioester reaction conformations, an observation that is supported by the recent solution of 4-chlorobenzoate•coenzyme A ligase crystal structure captured in both the adenylate-forming and the thioester-forming conformations.<sup>38</sup> Lacking a crystal structure of firefly luciferase trapped in the second, light producing configuration, Brachini et al. performed an experiment in which the N- and C-terminal domains were trapped in this arrangement by chemical crosslinking of two cysteine residues, one from each domain, with 1,2-bis(maleimidoethane). In the trapped configurational state, bioluminescence was not observed unless synthetic dehydroluciferyl-AMP substrate was added to bypass the inactivated adenylation half-step.<sup>39</sup> Analysis of the recently solved structure of this cross-linked firefly luciferase finds it locked into a conformation similar to the thioester formation step in acyl CoA synthetases.<sup>40</sup>

Based on these studies, it has been proposed that A-domains may adopt at least three conformations: an open conformation in the absence of substrates, the adenylation conformation upon the binding of an amino acid substrate and ATP, and the thioester conformation, a 140° rotation from the adenylation conformation, that occurs upon the release of PPi.<sup>34</sup> Both nocardicin synthetase initiation domains A1 and A4 and elongation domain A2 failed to catalyze an ATP/PPi exchange reaction in the presence of their preferred amino acid substrates until the addition of NocI.

Based on the studies described above, it is postulated that these domains can be “trapped” in a state in which one or more of the substrate-binding, adenylation, or thioester-forming conformations is blocked in a way that is relieved by NocI or other compatible MbtH protein. Expanding on this hypothesis, pull-down studies reported here support a 1:1 stoichiometric relationship between NocI and an interacting A-domain. In secondary metabolism, there is a set of glycosyltransferases (GTs) whose activity requires a stoichiometric amount of a partner protein for activity. DesVII, a GT involved in macrolide biosynthesis from *S. venezuelae*, requires DesVIII for activity and these two proteins were shown to form a tight 1:1 complex when co-purified.<sup>41</sup> Analogously, EryCIII a GT required for erythromycin D biosynthesis, requires partner protein EryCII for activity and the structure of the complex formed by these two proteins, a dimer of heterodimers, has been recently solved.<sup>42</sup> Analytical gel chromatographic analysis of the tyrosine adenylation enzyme SimH coupled to its cognate MbtH protein, SimY also indicates the formation of a heterotetrameric complex.<sup>20</sup> The EryCIII•EryCII interface is characterized where the N-terminal helix of EryCII is sitting in a groove formed by three helices in EryCIII and stabilized by electrostatic interactions. This observation suggests two roles for the partner protein EryCII, stabilization of the GT and allosteric regulation.<sup>42</sup> It appears that MbtH proteins also might share these two roles to varying degrees. While neither NocI nor NocP was required for the expression of modules from NocA or NocB in *E. coli*, the requirement for co-expression of a cognate MbtH protein with an NRPS protein domain in *E. coli* has

been reported in several cases suggesting a stabilization role for the MbtH protein in these instances.<sup>11,43–45</sup>

The ability to reconstitute the A-domain•MbtH protein interaction *in vitro* with separately expressed proteins has been evaluated. Measurements of A<sub>4</sub>T<sub>4</sub>-His<sub>6</sub> and A<sub>1</sub>T<sub>1</sub>-His<sub>6</sub> reconstituted with NocI, indicated ATP/PPi exchange activity of 50 – 70% of the activity observed for an equivalent amount of the co-expressed proteins. These differences in activity may be due to the presence of impurities or unfolded proteins, skewing the protein quantitation. Similar reconstitution experiments on different systems have shown varying results. The co-expression of CloH and CloY resulted in a protein mixture that was ~50% less active than the reconstitution of separately expressed proteins.<sup>20</sup> Conversely, the co-expressed proteins CmnO and CmnN resulted in a dramatically more active mixture than when the equivalent amounts of CmnO and CmnN from single expressions were combined.<sup>18</sup>

Of the three L-*p*HPG activating domains in NocA and NocB, only A1 is dependent on an MbtH protein for activation. Alignments of the nocardicin NRPS domains were performed to determine a conserved region that might be responsible for interaction with MbtH proteins (Supporting Information Figure S2). Based on alignment data of MbtH-dependent CloH and MbtH-independent NovH (83% identity), a single mutation, L383M was made in CloH resulting in a mutant protein with some MbtH-independent ATP/PPi exchange activity.<sup>20</sup> However, the position corresponding to CloH L383 in all the nocardicin A-domains as well as all other MbtH protein dependent A-domains (Supporting Information Figure S3) is a positively charged arginine residue (except for lysine in NocB A4), suggesting that the analogous mutation in A-domains other than CloH would not restore MbtH protein independent A-domain activity. Identification of a residue or set of residues that may account for the binding of NocI by A1, A2, and A4 but not A3 and A5 was not fruitful. A similar analysis, alignment of MbtH-independent L-Arg activating A6 domain from the lysobactin NRPS with the similar MbtH-dependent A2 domain from NocA (Supporting Information Figure S4) also failed to suggest a MbtH protein binding site. The observation that NocP substituted for NocI for A<sub>1</sub>T<sub>1</sub>-His<sub>6</sub> and A<sub>4</sub>T<sub>4</sub>-His<sub>6</sub> but not for MBP-A<sub>2</sub>T<sub>2</sub>-His<sub>6</sub> suggests variability at the A-domain•MbtH interface, complicating prediction of interaction sites.

The discovery of the MbtH protein requirement for ATP/PPi exchange activity has been crucial for furthering the understanding of nocardicin A biosynthesis. As noted earlier, the structure of the nocardicins is characterized by the nonribosomal tripeptide core D-*p*HPG–L-Ser–D-*p*HPG biosynthesized by NRPSs NocA and NocB comprising five modules, all essential for nocardicin A biosynthesis.<sup>46</sup> The heterologous expression and ATP/PPi exchange data for the modules of NocA and NocB validates the previous assumption that the tripeptide core derives from modules 3, 4 and 5.<sup>24</sup> The substrate specificities for MbtH-dependent A1 and A2, L-*p*HPG and L-Arg, respectively, have been of particular interest due to their absence in nocardicin A, and in the case of A2, the inability to predict its substrate using bioinformatics or establish it experimentally.

Both *in vivo* and *in vitro* experimental evidence collected on NocA+NocB is consistent with a linear NRPS producing pentapeptide L-*p*HPG–L-Arg–D-*p*HPG–L-Ser–L-*p*HPG instead of a “Type C” NRPS model in which module skipping occurs to yield a tripeptide, as suggested previously.<sup>24</sup> The trimming of leader peptides from ribosomal protein products is well known in nature, but there are only a few examples of proteolysis in the biosynthesis of nonribosomal natural products. The trimming of a leader peptide has been observed in xenocoumarin biosynthesis by periplasmic protease XcnG<sup>47</sup> and during didemnin biosynthesis by an unknown protease.<sup>48</sup> The excision of an N-terminal fatty acid chain



added by an NRPS in pyoverdine biosynthesis by periplasmic protease PvdQ has been demonstrated<sup>49</sup> while a similar reaction is suspected in saframycin biosynthesis.<sup>50</sup> Although tabtoxin is not a nonribosomal product, this  $\beta$ -lactam-containing pro-drug is trimmed by periplasmic peptidase, TapP to its active form.<sup>51</sup> The backbone of caerulomycin A is biosynthesized by a PKS-NRPS hybrid in which the terminal amino acid added in the final module, L-leucine, is removed later in the biosynthesis by a metallo-dependent amidohydrolase CrmL.<sup>52</sup>

The proteases discussed in the examples above, XcnG, PvdQ, TapP and CrmL are all encoded in their respective gene clusters. The only gene candidate resembling a protease in the nocardicin A gene cluster is NocK. NocK contains a catalytic triad consistent with a serine protease<sup>53</sup> and an N-terminal signal sequence predicting the export of this protein via the twin arginine translocation (Tat) pathway to periplasm.<sup>54,55</sup> However, the definitive assignment of a proteolytic role for NocK is compromised by insertional inactivation experiments showing that *nocK* is not essential for nocardicin A biosynthesis in *N. uniformis*.<sup>53</sup> While the timing of the cleavage of the leader peptide is currently unclear as is any role the leader dipeptide might have in downstream reactions, biosynthetic logic dictates that in nocardicin A biosynthesis, trimming of the N-terminal leader dipeptide occurs prior to oxime formation (catalyzed by NocL) at the N-terminus of the remaining tripeptide. Since the P450 catalyzed oxime reaction likely occurs in the cytoplasm, it seems unlikely that during nocardicin A biosynthesis, an intermediate would be exported to the periplasm for proteolysis requiring the tripeptide intermediate to be imported back to the cytoplasm for reaction with NocL.

The identification of L-Arg as the preferred substrate for A2 leads to the possibility that the pentapeptide core is trimmed during nocardicin A biosynthesis by an ordinary cytoplasmic trypsin-like protease (Scheme 1). While trypsin, a serine protease, is more commonly known as mammalian digestive enzyme, it has also been identified in a wide range of organisms including *Streptomyces*.<sup>29</sup> Analysis of the nocardicin A gene cluster, 15 kbp of the upstream nucleotide sequence and ~5 kbp of the downstream nucleotide sequence failed to elucidate a gene encoding a trypsin protease. Phylogenetic classification of the *N. uniformis* strain used in these studies based on 16S rDNA was performed to determine if *N. uniformis* was similar to the nocardicin A producing *A. mirum* strain that has been fully sequenced. Unexpectedly, the 16S rDNA of these two strains were found to be identical, supporting the previous observation that *N. uniformis* strain ATCC 21806 formed synnemata and zoospores highly similar to *A. mirum*.

A BLAST-P search of the *A. mirum* genome for proteins similar to the well characterized known *S. griseus* and *S. erythraeus* trypsins identified three proteins with greater than 38% identity and greater than 50% similarity and several others of lower identity and similarity.<sup>30,32</sup> The conserved catalytic triad and substrate specificity pocket characteristic of trypsin is observed in the protein sequence alignment of the putative *A. mirum* trypsin proteases.<sup>29</sup> (Supporting Information Figure S5) These proteins are not encoded in the defined nocardicin A gene cluster, but may be available to the nocardicin A biosynthetic pathway due to their constitutive expression or cross-talk between gene clusters as observed in the erythrochelin and rhodochelin biosynthetic pathways.<sup>56-58</sup> Cross-talk between gene clusters has been proposed to occur in *A. mirum* during the biosynthesis of the siderophore mirubactin.<sup>59</sup> The presence of trypsin and the ability of bovine trypsin to cleave the predicted pentapeptide product, L-*p*HPG-L-Arg-D-*p*HPG-L-Ser-L-*p*HPG, at the C-terminal site of the L-Arg residue, supports this hypothesis.

Although whole cell incorporation experiments with a linear peptide would likely result in proteolysis of the peptide by nutrient uptake systems, two experiments were performed in

which either peptide L-*p*HPG-L-Arg-D-*p*HPG-L-Ser-L-*p*HPG or its D-isomer peptide L-*p*HPG-L-Arg-D-*p*HPG-L-Ser-D-*p*HPG was added to the fermentation culture of a previously characterized *N. uniformis* point mutant, *nocB* S571A, in which the NRPS is inactivated. Unfortunately, nocardicin A production was not observed with either peptide but peaks correlated to 4-mer and 3-mer degradation products were observed, consistent with proteolytic degradation from the N-terminus.

An alternative, self-cleavage mechanism is also proposed in Scheme 1. Conversion of the second position L-Arg to L-Orn by an arginase could lead to cyclization by attack of the side chain amine of L-Orn on the amide carbonyl. This would result in self cleavage at the C-terminus of L-Arg, liberating the tripeptide core of the nocardicins as previously suggested.<sup>24</sup>

## Conclusion

In conclusion, MbtH protein dependence of A-domain activity was observed in A1, A2, and A4 of the nocardicin A NRPSs, while A3 and A5 showed no such requirement. The two MbtH proteins associated with or near the cluster were found to be not completely complementary, indicating that interaction with an A-domain is more complex than simple association with the three conserved tryptophan residues characteristic of MbtH proteins. Analysis of co-expressed protein complexes indicates a 1:1 stoichiometry between A-domains A1 and A4 with NocI. This discovery enabled the determination of the substrate amino acid specificity for each A-domain using the ATP/PPi exchange assay to yield a predicted product, L-*p*HPG-L-Arg-D-*p*HPG-L-Ser-L-*p*HPG, for the nocardicin NRPS. The requirement for truncation of this pentapeptide and the absence of a protease in the nocardicin A gene cluster that could perform such a function led to the proposal of a self-cleavage mechanism or the action of a protease encoded outside the gene cluster. Classical morphological criteria that have suggested *N. uniformis* ATCC 21806 should be reclassified as *A. mirum* were confirmed by direct comparison of their 16S rDNA sequences and the mutual identity of three candidate trypsin-encoding genes. Cross-talk with these enzymes or other endo- or exo- proteases can be invoked to account for truncation to the tripeptide core of the nocardicins. With the identity of a putative pentapeptide precursor in hand and the availability of a sequenced genome, the way is open to address the central timing and mechanistic questions of peptide processing,  $\beta$ -lactam formation, and C-terminal epimerization.

## Experimental Methods

### Cloning of NRPS Expression Vectors

The primers used for the PCR amplification of the coding region of each multi-domain construct are described in Table 1. Amplification from previously prepared plasmids was performed using Pfu (Agilent Technologies, Santa Clara, CA), Pfu Turbo (Agilent), or KOD (EMD Biosciences, Gibbstown, NJ) DNA polymerases. For modules 1 and 4, the PCR products were digested with *Nco*I and *Xho*I and directly ligated into the *Nco*I/*Xho*I site in pET28b(+) (EMD Biosciences). For modules 2, the PCR product was digested with *Nco*I and *Bam*H I and directly ligated into the *Nco*I/*Bam*H I site in pET28b(+). For cloning into pMALc2x (New England Biolabs, Ipswich, MA), the *Nco*I/*Blp*I fragment was excised from pET28b(+) blunted with a Klenow reaction and ligated into the Klenow blunted *Eco*R I/*Hind*III site of pMALc2x. The PCR product for module 3 was digested and directly ligated into the *Nco*I/*Bam*H I site of pQE60 (Qiagen, Valencia, CA). The module 3-histidine tag coding sequence was digested from pQE60 with *Nco*I/*Hind*III for ligation into the *Nco*I/*Hind*III site of pET28b(+). The PCR product encoding module 5 was subcloned into pCRblunt (Life Technologies, Grand Island, NY). The coding region was excised from

pCRBlunt with a *Nco*I/*Hind*III digest and ligated into the *Nco*I/*Hind*III site of pET28b(+). All constructs were confirmed by sequencing analysis performed by the Biosynthesis and Sequencing Facility, Johns Hopkins Medical School, Baltimore, MD.

### Cloning of *NocI* and *NocP* Expression Vectors

The *nocI* gene was amplified by PCR from cosmid DNA using KOD DNA polymerase and the primers listed in Table 2. PCR products were subcloned into pCRBlunt or pJET1.2 (ThermoFisher Scientific, Waltham, MA), confirmed by sequencing prior to excision and ligation into pCDFDuet (EMD Biosciences) and pTYB12 (New England Biolabs), respectively, using the cut sites indicated. The *nocP* gene was similarly amplified by PCR from cosmid DNA using KOD DNA polymerase and the primers listed in Table 2. PCR products were directly cloned into the *Nde*I/*Xho*I sites of pET28b(+) and pCDFDuet, respectively.

### Heterologous Expression and Purification of NRPS Modules

Seed cultures consisting of 50 mL LB medium with 25 ug/mL kanamycin for pET28 constructs or 100 ug/mL for pMALc2x constructs and 34 ug/mL chloramphenicol inoculated with *E. coli* BL21(DE3) Rosetta2 (EMD Biosciences) transformed with expression vector were grown overnight at 37 °C with shaking. The growth medium, 2xYT (3L) supplemented with 5 mM MgCl<sub>2</sub>, 25 ug/mL kanamycin or 100 ug/mL ampicillin, and 34 ug/mL chloramphenicol was inoculated with the seed culture at a ratio of 1:100. Cells were grown at 37 °C with shaking until the OD<sub>600</sub> measured ~ 0.6. Growth cultures were cooled to 17.5 °C prior to induction of protein expression with the addition of IPTG (1 mM final concentration for pET28b, 0.3mM for pMALc2x). Expression was continued overnight at 17.5 °C. Cells were collected by centrifugation (5180 × *g*, 10 min at 4 °C) then resuspended in lysis buffer (50 mM NaH<sub>2</sub>PO<sub>4</sub> pH = 8, 300 mM NaCl, 10 mM imidazole, 10% glycerol) and lysed by sonication. The cell debris was collected by centrifugation at 37044 × *g*, 4 °C for 30 min. NTA resin (Qiagen) was added to the lysate and allowed to incubate at 4 °C with turning for at least 1 h. The lysate-resin slurry was poured into an empty column. The resin was washed with lysis buffer followed by wash buffer (50 mM NaH<sub>2</sub>PO<sub>4</sub> pH = 8, 300 mM NaCl, 20 mM imidazole, 10% glycerol). The His<sub>6</sub> tagged protein was eluted with 4 – 10 mL elution buffer (50 mM NaH<sub>2</sub>PO<sub>4</sub> pH = 8, 300 mM NaCl, 250 mM imidazole, 10% glycerol).

Protein isolated by affinity chromatography was dialyzed in 3 × 1L dialysis buffer (50 mM Tris-HCl pH = 7.5 @ 4 °C, 50 mM NaCl, 5 mM MgCl<sub>2</sub>, 1 mM DTT, 10% glycerol), 1 h for each exchange. For further purification of modules 1, 3, 4, and 5, the protein solution was loaded onto a 5 mL HiTrapQ cartridge (GE Life Sciences, Pittsburgh, PA) pre-equilibrated with dialysis buffer (50 mM NaCl) using a ÄKTA FPLC (GE Life Sciences). Fractions were collected as the 50 – 500 mM NaCl (300mL total volume) gradient was applied to elute adsorbed proteins at a flow rate of ~1 mL/min with UV detection at 280 nm. Fractions (3 mL) were collected and analyzed by SDS-PAGE. Fractions containing the target fusion protein were collected, concentrated to > 2 mg protein/mL using a centrifugal filter (Millipore Corp., Billerica, MA), and flash frozen in liquid nitrogen for storage at –80 °C.

### Heterologous Expression and Isolation of untagged *NocI*

Seed cultures consisting of 50 mL LB medium with 100 ug/mL ampicillin were inoculated with *E. coli* BL21(DE3) transformed with the pTYB12/*nocI* expression vector and grown overnight at 37 °C with shaking. Six flasks, each containing 0.5 L LB medium with 100 ug/mL ampicillin and inoculated with 5 mL seed culture, were grown at 37 °C, 180 rpm until OD<sub>600</sub> ~ 0.6, then cooled to 10 °C (1 h). IPTG, final concentration 0.5 mM, was added to induce protein expression. Expression was continued at 17.5 °C overnight with shaking.

The following steps were performed at 4 °C. The next day, cells were pelleted by centrifugation (5180 × *g*, 10 min) then resuspended in 150 mL lysis buffer (20 mM Tris-HCl pH = 8, 500 mM NaCl, 1 mM EDTA). Cells were lysed by sonication and the cell debris was removed by centrifugation. Chitin resin (New England Biolabs #E6900S), 10 mL, was conditioned with ~110 mL column buffer (50 mM Tris-HCl pH = 8, 50 mM NaCl, 10% glycerol). The clarified cell lysate was passed through the chitin bead column at a flow rate of ~1 mL/min. The column was then washed with 100 mL column buffer. When the level of the wash buffer was close to the top of the resin, 20 mL cleavage buffer (100 mM DTT in column buffer) was added to the column. The column was capped and the resin was resuspended in the cleavage buffer and incubated at 4 °C for 72 h. The column eluate was collected. An additional 10 mL cleavage buffer was applied to the column, eluted, and combined with the previous eluate. The 30 mL of column eluate was filtered using an Amicon (Millipore Corp.) Ultra 30 kDa MWCO centrifuge filter. The flow-through was collected and concentrated using an Amicon Ultra 3 kDa MWCO filter. Native NocI (untagged) was flash frozen in liquid nitrogen for storage in the -80 °C freezer.

### Co-Expression of Module (His<sub>6</sub>-tagged) and NocI or NocP (untagged)

Each module expression plasmid (pET28/Mx or pMALc2x/M2) was co-transformed with pCDFDuet/*nocI* (untagged) into *E. coli* BL21(DE3) Rosetta 2 using standard electroporation protocols. Conditions for growth, expression, and isolation by NTA affinity chromatography were similar to those given for the heterologous expression of individual modules above, except that 50 µg/mL spectinomycin was added to the seed culture and growth culture medium to maintain selection for the pCDFDuet/*nocI* expression vector. In addition, NTA chromatography was the terminal step in the isolation, i.e. further purification by ion exchange chromatography was not done.

### ATP/PPi Exchange Assay

Each 100 µL reaction consisted of 36.3 mM HEPES pH = 7.5, 0.15 mM EDTA, 7.25 mM MgCl<sub>2</sub>, 1.5 mM DTT 3.7 mM ATP, 7.3% (v/v) glycerol, 0.75 mM amino acid substrate, and 1 mM Na<sub>4</sub>P<sub>2</sub>O<sub>7</sub> with 1 uCi <sup>32</sup>P-labeled Na<sub>4</sub>P<sub>2</sub>O<sub>7</sub> (NEN Perkin Elmer, Waltham, MA). The reaction was initiated by the addition of the protein (0.5–5 µM). Following incubation at room temperature for 30 min, the reaction was quenched by the addition of 400 µL 0.5M HClO<sub>4</sub>, chased with 400 µL 100 mM sodium pyrophosphate (unlabelled) and 200 µL of a 4% (w/v) suspension of activated charcoal (Norit A) was added. The charcoal was pelleted by centrifugation (14,000 rpm, 5 min), washed twice with 1 mL water and re-pelleted by centrifugation. The charcoal pellet was resuspended in 500 mL water, transferred to a 7 mL glass scintillation vial, and mixed with 5 mL of Optifluor (NEN Perkin Elmer). Each sample was measured using a Beckman model LS6500 scintillation counter (Beckman Coulter, Brea, CA).

### Modified ATP/PPi Exchange Assay for Module 2

Each 200 µL reaction mixture consisted of 50 mM Tris-HCl pH = 7.5, 10 mM MgCl<sub>2</sub>, 5 mM amino acid substrate, 2.5 mM Na<sub>4</sub>P<sub>2</sub>O<sub>7</sub> with 2 uCi <sup>32</sup>P-labeled Na<sub>4</sub>P<sub>2</sub>O<sub>7</sub>, and 5 µM protein. Prior to the addition of ATP, the reaction mixture was incubated at 30 °C for 10 min. Following this pre-incubation, 2.5 mM ATP was added to initiate the ATP/PPi exchange reaction was incubated at 30 °C for an additional 30 min. The exchange reaction was quenched with acid and prepared for scintillation counting using the procedure outlined in the previous section.

## Determination of Module:NocI Stoichiometry by HPLC

Samples isolated by NTA affinity chromatography were denatured by the addition of 8 M urea (Sigma-Aldrich, St. Louis, MO) to a final concentration of 6 M urea and incubated at room temperature for 30 min. Following incubation, samples were diluted with water for a final concentration of 2 M urea. Samples were analyzed by protein HPLC, employing an Agilent 1200 HPLC system equipped with a diode array detector. Filtered denatured protein solutions (100  $\mu$ L) in 2 M urea were injected onto a Vydac C4 protein column 150  $\times$  46 mm column (W.R. Grace & Co., Columbia, MD) heated to 70  $^{\circ}$ C. The flow rate was 1 mL/min. Proteins were eluted using a binary gradient in which mobile phase A consisted of 90:10 water : acetonitrile (ACN) with 0.1% trifluoroacetic acid (TFA) and mobile phase B consisted of 90:10 ACN : water with 0.1% (TFA). After 3 min at 82:18 A:B, a linear gradient to 50:50 A:B over 45 min was programmed. Proteins were detected by monitoring absorbance at 280 nm and were quantified by integration using OriginPro v.8.6 software (OriginLab, Northampton, MA). The molar absorptivity for each protein was calculated using Vector NTI software (Life Technologies).

## Conditions for Proteolysis and HPLC Analysis

Peptide L-*p*HPG-L-Arg-D-*p*HPG-L-Ser-L-*p*HPG was procured from Peptide 2.0, Inc. (Chantilly, VA) for testing. In a total reaction volume of 100  $\mu$ L, 200 nmol of pentapeptide was reacted with 20  $\mu$ g modified (TPCK-treated) trypsin (New England Biolabs) in buffer containing 50 mM Tris-HCl, pH = 8 @ 25  $^{\circ}$ C and 20 mM CaCl<sub>2</sub>. The reaction was incubated at 37  $^{\circ}$ C overnight. Trypsin was removed from the reaction by filtration through 3 kDa MWCO centrifugal filter (Millipore) and the flow-through was analyzed by an Agilent 1100 HPLC equipped with a diode array detector. Aliquots of the reaction mixture were injected onto a Luna C18(2) column (250 mm  $\times$  46 mm) (Phenomenex, Torrance, CA) using a binary gradient in which mobile phase A consisted of 0.1% trifluoroacetic acid (TFA) in water and mobile phase B consisted of 90:10 ACN : water with 0.1% (TFA). After 5 min at 94:6 A:B and a flow rate of 1 mL/min, a linear gradient to 85:15 A:B over 15 min was programmed.

LC-MS analysis was conducted using an Agilent 1200 series, 6220 LC/MS TOF analyzer equipped with a dual ESI source operated in positive mode under the following conditions: fragmentor: 135 V, skimmer: 65 V, gas temperature: 350  $^{\circ}$ C, drying gas: 12 L/min, nebulizer 40 psi and Vcap: 3500 V for mass range 100 to 1700 m/z. Separations were performed with a Zorbax C18 5 micron column (150 mm  $\times$  4.6 mm) at 30  $^{\circ}$ C using a binary gradient in which mobile phase A consisted of 0.1% formic acid in water and mobile phase B consisted of 90:10 ACN : water with 0.1% formic acid. A linear gradient elution from 6% to 85% mobile phase B over 15 min was programmed. An aliquot of the trypsin reaction mixture described above was diluted 1:100 with 0.1% formic acid in water and 5  $\mu$ L was injected for LC-MS analysis.

## Pentapeptide Feeding Experiment

The preparation and growth conditions for the *N. uniformis nocB* S571A mutant has been described previously.<sup>46</sup> *N. uniformis* is maintained on ISP2 solid medium (Difco Laboratories, Detroit, MI) at 28  $^{\circ}$ C. Seed cultures were prepared in TSB medium (Difco Laboratories) and grown to saturation at 28  $^{\circ}$ C with shaking. Nocardicin fermentation medium<sup>60</sup> was inoculated with 2 mL of the starter seed culture and incubated at 28  $^{\circ}$ C with shaking. Following 34 h of incubation, the culture medium was supplemented with peptide L-*p*HPG-L-Arg-D-*p*HPG-L-Ser-L-*p*HPG or peptide L-*p*HPG-L-Arg-D-*p*HPG-L-Ser-D-*p*HPG (Peptide 2.0, Inc., Chantilly, VA) to a final concentration of 5 mM. The supplemented mutant *N. uniformis* cultures were incubated for an additional day. Upon completion, the cultures were centrifuged to separate the cell mass from the supernatant,

analyzed by HPLC, and stored at  $-20^{\circ}\text{C}$ . HPLC analysis to detect nocardicin A was performed as described previously.<sup>46</sup> A second HPLC analysis for the detection of novel metabolites was performed using the same HPLC system and Luna C18(2) column (Phenomenex, Torrance, CA). For this analysis, the binary mobile phase solutions were: A: 0.1% trifluoroacetic acid (TFA) in water and B: 90:10 acetonitrile:water with 0.1% TFA. Filtered culture supernatants (10  $\mu\text{L}$ ) were directly injected and eluted with a shallow gradient starting with a ratio of 94:6 (A:B) for 5 min, to a ratio of 85:15 (A:B) at 20 min and ending with a ratio of 60:40 (A:B) at 40 min. Analytes were detected at 272 nm with a diode array detector.

### Phylogenetic Analysis of *N. uniformis* ATCC 21806

The isolation of genomic DNA from *Nocardia uniformis* subsp. *tsuyamanensis* ATCC 21806 was carried out according to the standard techniques from *Practical Streptomyces Genetics*.<sup>61</sup> Amplification of 16S rDNA in was performed using the universal 16S rDNA primers fd1 and rp2<sup>62</sup> with KOD DNA polymerase. PCR products were sub-cloned into pJET1.2 and submitted for sequencing at the Biosynthesis and Sequencing Facility, Johns Hopkins Medical School, Baltimore, MD. The resulting sequences were compared with those available in the GenBank database maintained by the National Center for Biotechnology Information (NCBI) using the BLASTN algorithm.<sup>30</sup>

### PCR Amplification of Trypsin Coding Sequences from *N. uniformis*

Using the Primer-BLAST<sup>63</sup> algorithm on the NCBI website, primers (Table 3) were designed to amplify regions encoding three trypsin proteases predicted to be present in *N. uniformis* based on the *A. mirum* genome. Targeted genes were amplified from gDNA isolated *N. uniformis* using KOD DNA polymerase. PCR products were sub-cloned into pJET1.2 and submitted for sequencing analysis.

### Supplementary Material

Refer to Web version on PubMed Central for supplementary material.

### Acknowledgments

This work was supported by NIH grant AI014937. The Greenberg group (JHU) is thanked for use of their FPLC and support for radiochemical experiments. Dr. W.E. Bocik performed the initial sub-cloning of *nocI* and we thank Prof. D. I. Barrick (Biophysics, JHU) for helpful discussions. Prof. P. F. Leadlay (Cambridge) kindly provided samples of L- $\delta$ -*N*-hydroxyornithine and L- $\delta$ -*N*-acetyl- $\delta$ -*N*-hydroxyornithine for the ATP/PPi exchange assays. Drs. A. C. Jacobs and I. P. Mortimer are acknowledged for their help with MALDI and ESI-MS measurements. Mr. E. Philander (Analytical Sciences Group, McCormick & Co., Inc.) kindly performed the LC-MS analyses described in this manuscript.

### References

1. Felnagle EA, Jackson EE, Chan YA, Podevels AM, Berti AD, McMahon MD, Thomas MG. *Mol Pharmaceutics*. 2008; 5:191–211.
2. Lai JR, Fischbach MA, Liu DR, Walsh CT. *J Am Chem Soc*. 2006; 128:11002–11003. [PubMed: 16925399]
3. Walsh C, Chen H, Keating T, Hubbard B, Losey H, Luo L, Marshall C, Miller D, Patel H. *Curr Op Chem Biol*. 2001; 5:525–534.
4. Sattely ES, Fischbach MA, Walsh CT. *Nat Prod Rep*. 2008; 25:757–793. [PubMed: 18663394]
5. Hahn M, Stachelhaus T. *Proc Natl Acad Sci USA*. 2004; 101:15585–15590. [PubMed: 15498872]
6. Quadri LEN, Sello J, Keating TA, Weinreb PH, Walsh CT. *Chem Biol*. 1998; 5:631–645. [PubMed: 9831524]

7. Lautru S, Oves-Costales D, Pernodet J-L, Challis GL. *Microbiology*. 2007; 153:1405–1412. [PubMed: 17464054]
8. Wolpert M, Gust B, Kammerer B, Heide L. *Microbiology*. 2007; 153:1413–1423. [PubMed: 17464055]
9. Drake EJ, Cao J, Qu J, Shah MB, Straubinger RM, Gulick AM. *J Biol Chem*. 2007; 282:20425–20434. [PubMed: 17502378]
10. Buchko GW, Kim C-Y, Terwilliger TC, Myler PJ. *Tuberculosis*. 2010; 90:245–251. [PubMed: 20434955]
11. Heemstra JR, Walsh CT, Sattely ES. *J Am Chem Soc*. 2009; 131:15317–15329. [PubMed: 19778043]
12. Conti E, Stachelhaus T, Marahiel MA, Brick P. *The EMBO Journal*. 1997; 16:4174–4183. [PubMed: 9250661]
13. Challis GL, Ravel J, Townsend CA. *Chem Biol*. 2000; 7:211–224. [PubMed: 10712928]
14. Stachelhaus T, Mootz HD, Marahiel MA. *Chem Biol*. 1999; 6:493–505. [PubMed: 10421756]
15. Rausch C, Weber T, Kohlbacher O, Wohlleben W, Huson DH. *Nucl Acids Res*. 2005; 33:5799–5808. [PubMed: 16221976]
16. Röttig M, Medema MH, Blin K, Weber T, Rausch C, Kohlbacher O. *Nucl Acids Res*. 2011; 39:W362–W367. [PubMed: 21558170]
17. Prieto C, García-Estrada C, Lorenzana D, Martín JF. *Bioinformatics*. 2012; 28:426–427. [PubMed: 22130593]
18. Felnagle EA, Barkei JJ, Park H, Podevels AM, McMahon MD, Drott DW, Thomas MG. *Biochemistry*. 2010; 49:8815–8817. [PubMed: 20845982]
19. Zhang W, Heemstra JR, Walsh CT, Imker HJ. *Biochemistry*. 2010; 49:9946–9947. [PubMed: 20964365]
20. Boll B, Taubitz T, Heide L. *J Biol Chem*. 2011; 286:36281–36290. [PubMed: 21890635]
21. Watanabe K, Okuda T, Yokose K, Furumai T, Maruyama HB. *J Antibiot*. 1983; 36:321–324. [PubMed: 6833153]
22. Hasegawa T, Lechevalier MP, Lechevalier HA. *Int J Syst Bacteriol*. 1978; 28:304–310.
23. Townsend CA, Brown AM. *J Am Chem Soc*. 1983; 105:913–918.
24. Gunsior M, Breazeale SD, Lind AJ, Ravel J, Janc JW, Townsend CA. *Chem Biol*. 2004; 11:927–938. [PubMed: 15271351]
25. Rausch C, Hoof I, Weber T, Wohlleben W, Huson DH. *BMC Evol Biol*. 2007; 7:78. [PubMed: 17506888]
26. Hou J, Robbel L, Marahiel Mohamed A. *Chem Biol*. 2011; 18:655–664. [PubMed: 21609846]
27. Schlager R, Simmon KE, Fisher MA. *Emerg Infect Dis*. 2012; 18:422–430. [PubMed: 22377371]
28. Drancourt M, Bollet C, Carlizot A, Martelin R, Gayral J-P, Raoult D. *J Clin Microbiol*. 2000; 38:3623–3630. [PubMed: 11015374]
29. Rypniewski WR, Perrakis A, Vorgias CE, Wilson KS. *Protein Eng*. 1994; 7:57–64. [PubMed: 8140095]
30. Altschul S, Madden T, Schaffer A, Zhang J, Zhang Z, Miller W, Lipman D. *Nucl Acids Res*. 1997; 25:3389–3402. [PubMed: 9254694]
31. Stosová Tá, Sebela M, Rehulka P, Sedo O, Havlis J, Zdráhal Z. *Anal Biochem*. 2008; 376:94–102. [PubMed: 18261455]
32. Kiser JZ, Post M, Wang B, Miyagi M. *J Proteome Res*. 2009; 8:1810–1817. [PubMed: 19231893]
33. Drake EJ, Nicolai DA, Gulick AM. *Chem Biol*. 2006; 13:409–419. [PubMed: 16632253]
34. Yonus H, Neumann P, Zimmermann S, May JJ, Marahiel MA, Stubbs MT. *J Biol Chem*. 2008; 283:32484–32491. [PubMed: 18784082]
35. Du L, He Y, Luo Y. *Biochemistry*. 2008; 47:11473–11480. [PubMed: 18847223]
36. Osman KT, Du L, He Y, Luo Y. *J Mol Biol*. 2009; 388:345–355. [PubMed: 19324056]
37. Mitchell CA, Shi C, Aldrich CC, Gulick AM. *Biochemistry*. 2012; 51:3252–3263. [PubMed: 22452656]

38. Reger AS, Wu R, Dunaway-Mariano D, Gulick AM. *Biochemistry*. 2008; 47:8016–8025. [PubMed: 18620418]
39. Branchini BR, Rosenberg JC, Fontaine DM, Southworth TL, Behney CE, Uzasci L. *J Am Chem Soc*. 2011; 133:11088–11091. [PubMed: 21707059]
40. Sundlov JA, Fontaine DM, Southworth TL, Branchini BR, Gulick AM. *Biochemistry*. 2012; 51:6493–6495. [PubMed: 22852753]
41. Borisova SA, Liu H-w. *Biochemistry*. 2010; 49:8071–8084. [PubMed: 20695498]
42. Moncrieffe MC, Fernandez M-J, Spiteller D, Matsumura H, Gay NJ, Luisi BF, Leadlay PF. *J Mol Biol*. 2012; 415:92–101. [PubMed: 22056329]
43. Imker HJ, Krahn D, Clerc J, Kaiser M, Walsh CT. *Chem Biol*. 2010; 17:1077–1083. [PubMed: 21035730]
44. Zolova OE, Garneau-Tsodikova S. *MedChemComm*. 2012; 3:950–955.
45. McMahon MD, Rush JS, Thomas MG. *J Bacteriol*. 2012; 194:2809–2818. [PubMed: 22447909]
46. Davidsen JM, Townsend CA. *Chem Biol*. 2012; 19:297–306. [PubMed: 22365611]
47. Reimer D, Pos KM, Thines M, Grun P, Bode HB. *Nat Chem Biol*. 2011; 7:888–890. [PubMed: 21926994]
48. Xu Y, Kersten RD, Nam SJ, Lu L, Al-Suwailim AM, Zheng HJ, Fenical W, Dorrestein PC, Moore BS, Qian PY. *J Am Chem Soc*. 2012; 134:8625–8632. [PubMed: 22458477]
49. Drake EJ, Gulick AM. *ACS Chem Biol*. 2011; 6:1277–1286. [PubMed: 21892836]
50. Koketsu K, Watanabe K, Suda H, Oguri H, Oikawa H. *Nat Chem Biol*. 2010; 6:408–410. [PubMed: 20453862]
51. Levi C, Durbin RD. *Physiol Mol Plant Pathol*. 1986; 28:345–352.
52. Zhu YG, Fu P, Lin QH, Zhang GT, Zhang HB, Li SM, Ju JH, Zhu WM, Zhang CS. *Org Lett*. 2012; 14:2666–2669. [PubMed: 22591508]
53. Kelly WL, Townsend CA. *J Bacteriol*. 2005; 187:739–46. [PubMed: 15629944]
54. Petersen TN, Brunak S, von Heijne G, Nielsen H. *Nat Meth*. 2011; 8:785–786.
55. Bendtsen J, Nielsen H, Widdick D, Palmer T, Brunak S. *BMC Bioinf*. 2005; 6:167.
56. Lazos O, Tosin M, Slusarczyk AL, Boakes S, Cortés J, Sidebottom PJ, Leadlay PF. *Chem Biol*. 2010; 17:160–173. [PubMed: 20189106]
57. Robbel L, Helmetag V, Knappe TA, Marahiel MA. *Biochemistry*. 2011; 50:6073–6080. [PubMed: 21650455]
58. Bosello M, Robbel L, Linne U, Xie X, Marahiel MA. *J Am Chem Soc*. 2011; 133:4587–4595. [PubMed: 21381663]
59. Giessen TW, Franke KB, Knappe TA, Kraas FI, Bosello M, Xie X, Linne U, Marahiel MA. *J Nat Prod*. 2012; 75:905–914. [PubMed: 22578145]
60. Reeve AM, Breazeale SD, Townsend CA. *J Biol Chem*. 1998; 273:30695–30703. [PubMed: 9804844]
61. Kieser, T.; Bibb, MJ.; Buttner, MJ.; Chater, KF.; Hopwood, DA. *Practical Streptomyces Genetics*. The John Innes Foundation; Norwich UK: 2000.
62. Weisburg WG, Barns SM, Pelletier DA, Lane DJ. *J Bacteriol*. 1991; 173:697–703. [PubMed: 1987160]
63. Ye J, Coulouris G, Zaretskaya I, Cutcutache I, Rozen S, Madden T. *BMC Bioinf*. 2012; 13:134–145.



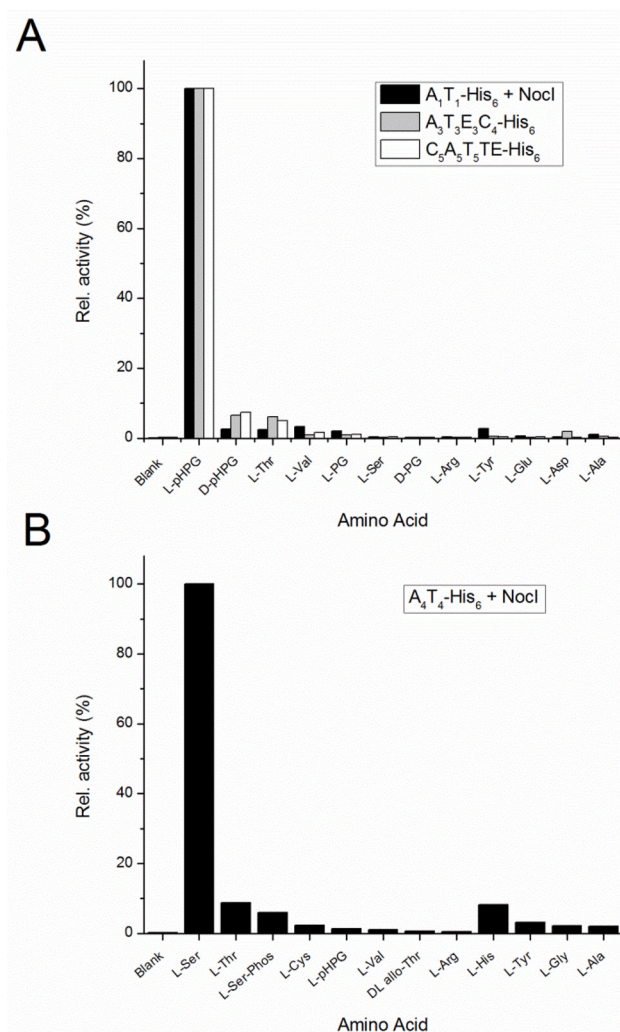


**Figure 1.** Representative results of the ATP/PPi exchange assay for L-pHPG activating modules A<sub>1</sub>T<sub>1</sub>-His<sub>6</sub>, A<sub>3</sub>T<sub>3</sub>E<sub>3</sub>C<sub>4</sub>-His<sub>6</sub> and C<sub>5</sub>A<sub>5</sub>T<sub>5</sub>TE-His<sub>6</sub> and L-serine activating module, A<sub>4</sub>T<sub>4</sub>-His<sub>6</sub> at 0.5uM. For modules A<sub>1</sub>T<sub>1</sub>-His<sub>6</sub> and A<sub>4</sub>T<sub>4</sub>-His<sub>6</sub> which require addition of a MbtH protein for activity, His<sub>6</sub>-Nocl was added at 2 uM final concentration. All assays were performed at room temperature.

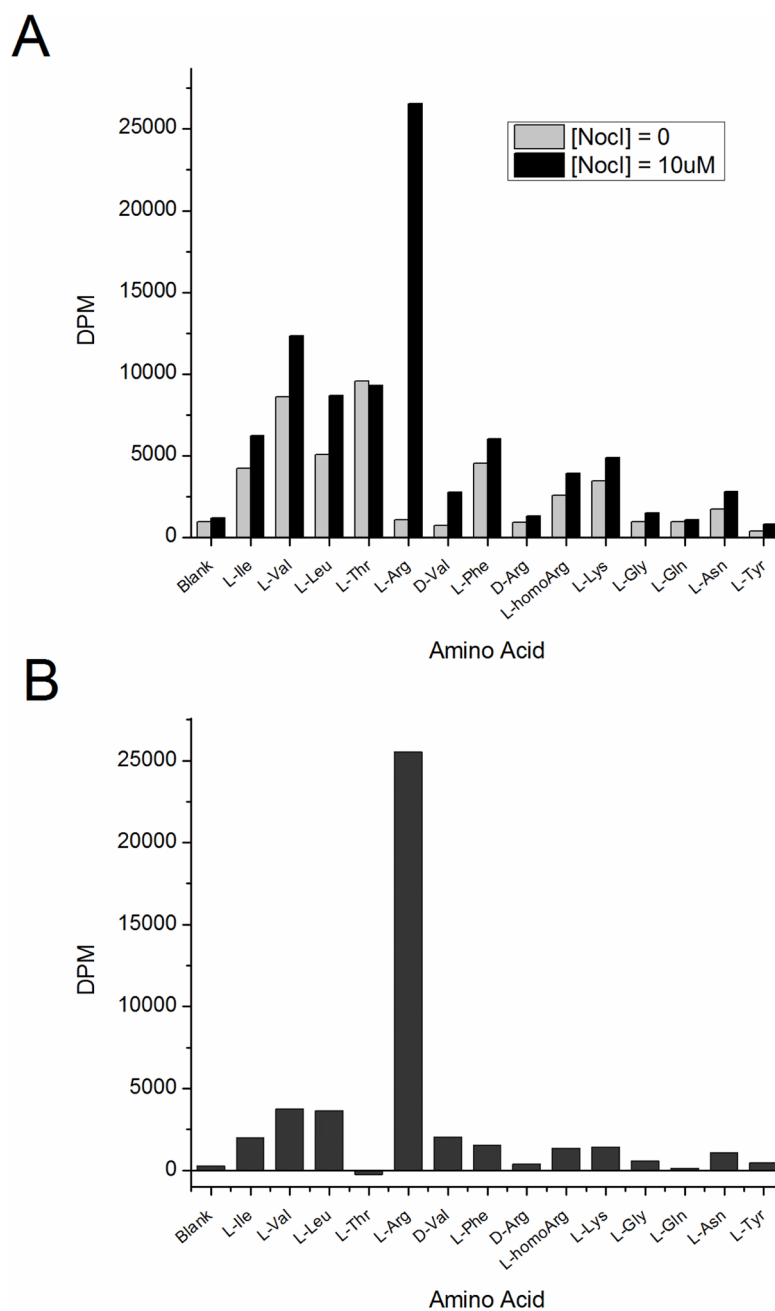


**Figure 2.** Representative results of the ATP/PP<sub>i</sub> exchange assay for 5 μM of the L-Arg activating MBP-A<sub>2</sub>T<sub>2</sub>-His<sub>6</sub> performed at 30 °C. A. Data plot for activity with and without addition of 10 μM His<sub>6</sub>-NocI. B. Difference plot – the activity of MBP-A<sub>2</sub>T<sub>2</sub>-His<sub>6</sub> with His<sub>6</sub>-NocI with the background activity seen in the absence His<sub>6</sub>-NocI subtracted.

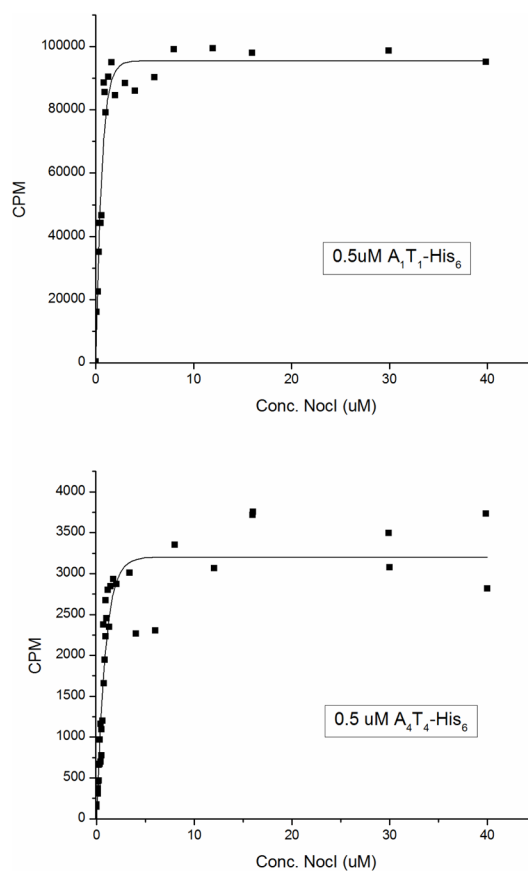


**Figure 3.** ATP/PPi exchange rate for modules A<sub>1</sub>T<sub>1</sub>-His<sub>6</sub> (A) and A<sub>4</sub>T<sub>4</sub>-His<sub>6</sub> (B) as a function of increasing NocI (untagged) concentration. The fitted line was generated by curve fitting to the Box Lucas model equation:  $y = a(1 - b^x)$  using OriginLab software version 8.6.

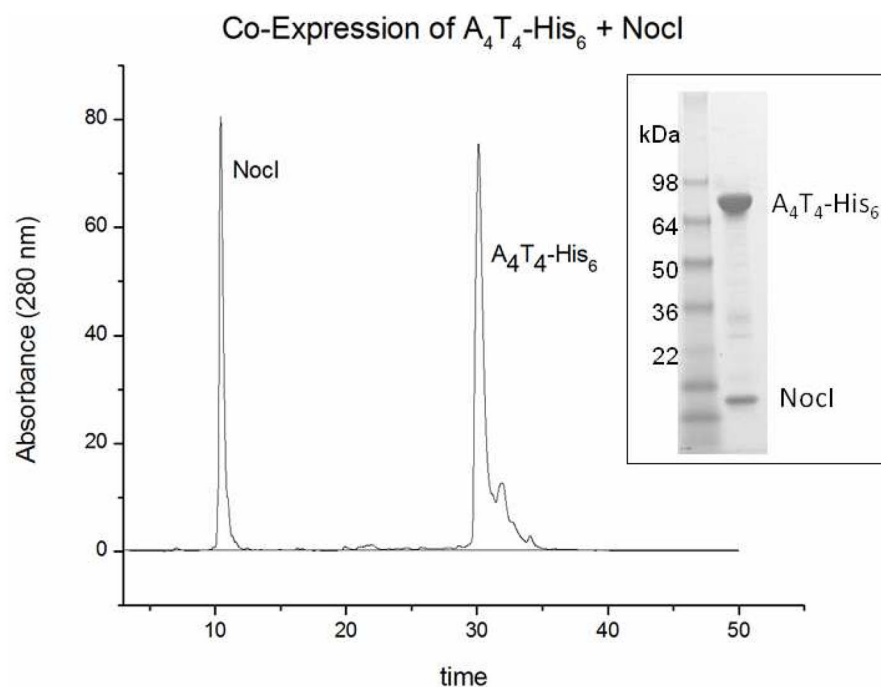
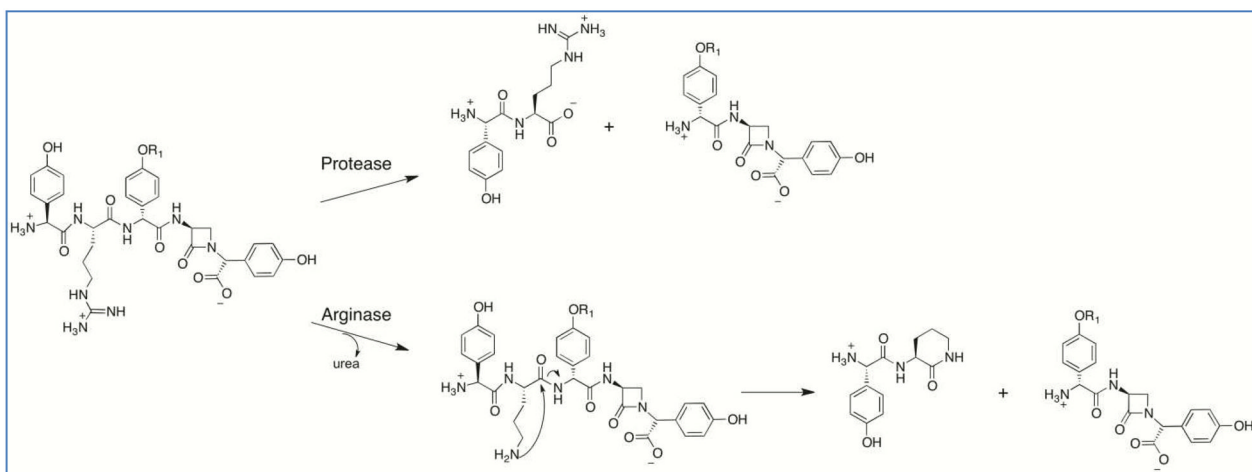


**Figure 4.** HPLC chromatogram and SDS-Page gel (inset) of  $A_4T_4$ -His<sub>6</sub>-NocI (untagged) coexpression, purified by NTA affinity chromatography.



**Scheme 1.**

**Table 1**

Oligonucleotide primers used for NRPS expression vector construction.

Description	Label	Primer Sequence (5' to 3')
A <sub>1</sub> T <sub>1</sub>	M1 For ( <i>Nco</i> I)	GCGCCATGGGGGACAGCGAGGAGTGGGAGCGC
	M1 Rev ( <i>Xho</i> I)	GCGCTCGAGGGCCAGCTCCTCGATCCGCCTGGCCAG
A <sub>2</sub> T <sub>2</sub>	M2 For ( <i>Nco</i> I)	GCCCATGGTTAGCACCGCGCGCCGGTCAACC
	M2 Rev ( <i>Bam</i> H I)	GCGGATCCCGCGTCGTCGGCCACGGC
A <sub>3</sub> T <sub>3</sub> E <sub>3</sub> C <sub>4</sub>	M3 For ( <i>Nco</i> I)	TCTTCCATGGTGCTCGGGGACGAC
	M3 Rev ( <i>Bam</i> H I)	TATAGGATCCCGGGTTCCTTCTCCCCTCG
A <sub>4</sub> T <sub>4</sub>	M4 For ( <i>Nco</i> I)	GCCCATGGCCTTTCGAGTGC GCGACCTGTTCCGGC
	M4 Rev ( <i>Xho</i> I)	GGCTCGAGGGTGGACGCCTCGTCGGCG
C <sub>5</sub> A <sub>5</sub> T <sub>5</sub> TE	M5 For ( <i>Nco</i> I)	GCGCTCCATGGACGAGGAGGCGCTGCTGGCG
	M5 Rev	TATAAAGCTCCGCTCCTCCAGCGCGC

**Table 2**

Oligonucleotide primers used for NocI and NocP expression vector construction.

Vector	Label	Primer Sequence (5' to 3')
pCDFDuet	NocI For ( <i>Nco I</i> )	GCC <u>CC</u> ATGGTGGGAGAGAACGAGGATTCCGG
	NocI Rev ( <i>Hind III</i> )	GCGAAGCTTTCAAGCCCGGTCCCCGGCC
pTYB12	NocI For ( <i>Bsm I</i> )	GCCGAATGCTCTGGGAGAGAACGAGGATTCCGG
	NocI Rev ( <i>Xho I</i> )	GCGCTCGAGTCAAGCCCGGTCCCCGGCC
pET28b(+)	NocP For ( <i>Nde I</i> )	GCGGCATATGAACCCCTTCGACGACCACGACCGCGT
	NocP Rev ( <i>Xho I</i> )	GCGCTCGAGTCAGGCGTCGGGGTCGGGCGCGCCCGCGG
pCDFDuet	NocP For ( <i>Nde I</i> )	GCGGCATATGAACCCCTTCGACGACCACGACCGCGT
	NocP Rev ( <i>Xho I</i> )	GCGCTCGAGTCAGGCGTCGGGGTCGGGCGCGCCCGCGG

**Table 3**

Trypsin Primer Sets	Primer Sequence (5' to 3')
ACU39320 - Forward	GGACATTGCGGTGGTGAAGACGTC
ACU39320 - Reverse	GGAAGGAGATGAGCATGGCGGAAACC
ACU39665 - Forward	CGCGCTCAGCACGCTGTAGTAGG
ACU39665 - Reverse	GAAAGGAACTCCGATGGCGAAAACCT
ACU39678 - Forward	CATCAGAGTCCGCATACCGCCAAC
ACU39678 - Reverse	ATCGACCTGGTCTTTCAGGGCTAACCT